Three-Component Solids Velocity Measurements in the Outlet Section of a Riser

Maria N. Pantzali, Javier Marqués de Marino, Guy B. Marin, and Geraldine J. Heynderickx
Laboratory for Chemical Technology, Faculty of Engineering and Architecture, Ghent University, Ghent, Belgium

DOI 10.1002/aic.15277
Published online May 6, 2016 in Wiley Online Library (wileyonlinelibrary.com)

Coincident (simultaneous) three-component particle velocity measurements performed using two laser Doppler anemometry probes at the outlet section of a 9 m high cylindrical riser are for the first time presented for dilute flow conditions. Near the blinded extension of the T-outlet a solids vortex is formed. Particle downflow along the riser wall opposite the outlet tube is observed, which is restricted to higher riser heights at higher gas flow rates. Increased velocity fluctuations are observed in the solids vortex and downflow region as well as at heights corresponding to the outlet tube. Contrary to the rest of the riser, in the downflow region time and ensemble velocity averages are not equal. Given the local bending of the streamlines, axial momentum transforms to radial and azimuthal momentum giving rise to the corresponding shear stresses. Turbulence intensity values indicate the edges of the downflow region. © 2016 The Authors AIChE Journal published by Wiley Periodicals, Inc. on behalf of American Institute of Chemical Engineers *AIChE J*, 62: 3575–3584, 2016

Keywords: fluidization, hydrodynamics, fluid mechanics, multiphase flow, riser

Introduction

The hydrodynamics of riser flows were extensively studied over the last decades due to the wide use of risers in industry.[1] The geometry of the outlet section is often found to significantly affect the flow and the cross-sectional solids concentration profile in the riser. Riser outlet geometries are characterized either as smooth, with a gentle exit curvature, or as abrupt.[2] It is generally observed that a smooth or weak restriction outlet hardly influences the flow, while an abrupt or strong restriction elbow results in solids recirculation and hence a significant decrease of the axial voidage and increase of pressure drop in the riser outlet section.[3–6] A smooth exit can promote less back-mixing and a more uniform residence time of particles, which is beneficial for riser cracking or fast pyrolysis reactors,[2] while an abrupt exit could increase the solids residence time and the heat transfer, as desired in combustion processes.[2,7] Higher flow resistance as well as slip velocities are reported for abrupt exits.[8] The solids distribution is found to vary significantly with solids flux.[9] Depending on the particle terminal velocities, the riser and outlet geometries, the recirculation caused by a strongly restrictive outlet may extend throughout the riser, particularly for risers with a height to diameter ratio below 5.[10,11] However, predicting the extent of these outlet effects remains difficult.[7] Correlations determining an optimal ratio of gas to solid velocities in risers with a strongly restrictive outlet have at best a limited accuracy of about ±40%.[5] Monazam et al.[6] recently claimed that the apparent voidage in the vicinity of a T-outlet is independent of the superficial gas velocity. Kim et al.[12] showed that at relatively high gas velocities a smooth (C) outlet can result in much higher solids fractions near the outlet section as compared to more abrupt (L and T) outlets. Chew et al.[13] reported that the core-annular flow in the lower and middle part of a riser can change to a reverse core-annular pattern close to the outlet for Geldart B particles. This is related to the high particle Stokes number (or high inertia) which allows for more diffused particle trajectories rather than particles following the fluid streamlines. Most experimental work in riser outlet sections focuses on measurements of pressure drop, solids distributions and solids fluxes.[2,3,7–15] Studies reporting solids velocities are limited and mostly reveal either one or two coincident components of the solids velocities or the overall velocity magnitude.[9,16,17] Detailed coincident three velocity components at the riser outlet section have been reported in literature for relatively high solids fluxes.[16,18,19]

Significant effort is focused on modeling riser gas–solid flows.[20–23] However the large riser domains and the complexity of the two-phase gas–solid flow result in an enormous computational load for three-dimensional (3D) riser simulations. Hence model as well as domain simplifications are necessary.[24] In most of the riser simulations the two-fluid model is combined with a two-dimensional (2D) domain to minimize the computational load. These simplifications can be adequate for predicting the flow through fluidized beds and in the middle section of a riser tube.[25–27] In the inlet and outlet section of a riser, however, the flow is highly anisotropic and 3D

Additional Supporting Information may be found in the online version of this article.

Correspondence concerning this article should be addressed to G. J. Heynderickx at geraldine.heynderickx@ugent.be.

effects need to be accounted for to obtain reliable simulation results.[25,28] Lately many researchers are focusing their computational work on the effect of the riser outlet geometry and often report contradictory trends.[29–31] Shi et al.[31] highlight the importance of carefully specifying the riser outlet geometry in any riser modeling study. The Energy-Minimization Multi-Scale (EMMS) model is reported by several researchers to be more adequate for simulations at the outlet, as the structural homogeneity assumption of traditional two-fluid models does not hold for flow close to the outlet.[8,30,32] The need for 3D simulations to capture the outlet effects of abrupt configurations has been repeatedly reported.[28,33,34] For dilute, turbulent flow the success of two-fluid modeling strongly depends on the applied closure models. As no Eulerian model is generally found to be acceptable, considerable efforts to develop more robust closure models and more appropriate wall functions are carried out.[35,36] Passalacqua and Fox[37] claim that two-fluid models are not capable of predicting dilute gas-solid flows, as particle trajectory crossings cannot be simulated while the simulation result becomes grid-dependent. To develop more appropriate closure models and wall models applicable for dilute flow, extensive sets of accurate experimental velocity data are required for validation purposes, which, to the authors' best knowledge, are hard to find in literature, especially in the inlet and outlet section of risers.

Research on more dilute riser flow in the Laboratory for Chemical Technology was initiated in a study of the SO_2-NO_x Adsorption Process (SNAP) flow.[38] The present work focuses on dilute flow in the strongly restrictive outlet section of a pilot riser. For the first time a very detailed statistical analysis of the solids velocity data is provided, making the whole set of data even more interesting for validation purposes. Finally, the experimental data presented in this article complete the experimental data, obtained under the same operating conditions, by Pantzali et al.[39] for the middle section and by Pantzali et al.[40] for the bottom section of the same pilot riser set-up. Combining the three papers thus results in a full picture of the three component solids velocity field in the entire riser.

Experimental Set-Up and Conditions

In this study, a cylindrical Pyrex glass riser 9 m high and 0.1 m in diameter is used. A detailed description of the circulating fluidized bed (CFB) pilot unit as presented in Figure 1 and its operating conditions have already been extensively discussed.[38–40] In view of presenting the data a cylindrical coordinate system (r,θ,z) is introduced with the origin (0,0,0) in the center point of the ring, where the gas, humidified air, expands to the riser diameter (Figure 1). The riser has a blinded T-outlet with a 0.1 m diameter and a 0.13 m extension height, positioned in the $\theta = 51°$ plane. The outlet opening extends from $z = 8.66$ m to $z = 8.76$ m. The solids used are FCC-E catalyst particles with a density of 1550 kg/m^3 and a mean diameter of 73 μm, classified as Geldart Group A particles.[41] The particle-size distribution and corresponding statistical characteristics can be found in Figure 2. The riser operates at atmospheric conditions and in "cold flow." Experimental data are gathered for volumetric air flow rates of 100 Nm^3/h and 150 Nm^3/h, corresponding with a superficial air velocity in the riser of 3.5 m/s and 5.3 m/s, respectively. The solids flux rate in the riser is kept constant at 1 kg/m^{2}s, implying that the mean solids volume fraction, ε_s, is less than 0.0002 and the mass loading, m, is less than 0.24 for all experiments. It should be noted however that these values will be significantly higher

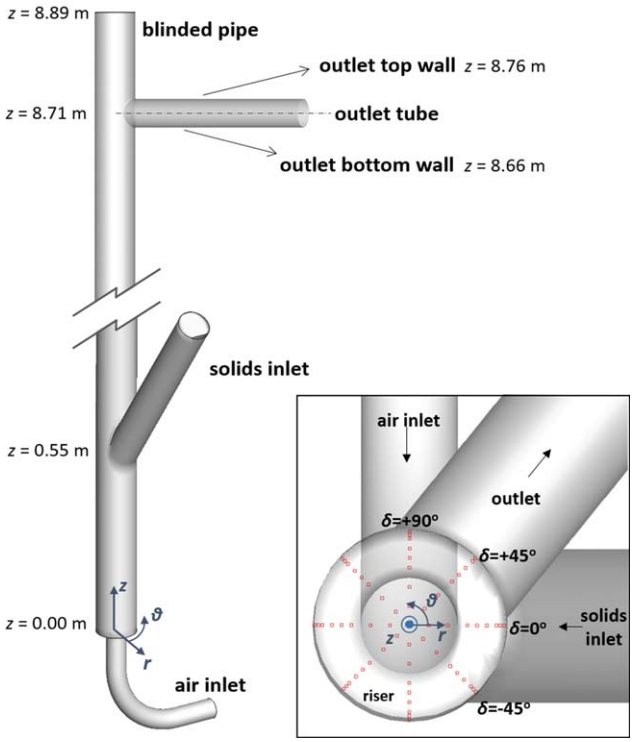

Figure 1. Schematic representation of the riser inlet and outlet section and of the riser $r\theta$ cross-section, where the measuring positions are indicated.[39].

[Color figure can be viewed in the online issue, which is available at wileyonlinelibrary.com.]

in the riser outlet section where the solids flow is disturbed by the outlet configuration and a solids reflux is observed.

The experimental set-up is equipped with a two-probe laser Doppler anemometer (LDA). A single LDA probe records one or maximum two components of particle velocities in a two-phase flow. The measuring volume dimensions are of the order of 150 μm, indicating that each measurement is spatially confined. Using two LDA probes positioned in a proper orientation with respect to the riser allows recording all three orthogonal components of the solids velocities in the gas–solid two-phase flow simultaneously. This is referred to as coincident solids velocity measurements. By repositioning the probes and measuring at various positions, particle velocities profiles are acquired. More details can be found in Pantzali et al.[39] The probes are positioned on a $r\theta$ plane with a 90° angle in between them. They are fixed on a traverse manifold that enables to reposition the measuring volume relatively to the riser cross-section, stepwise and accurately. The LDA with the traverse manifold is placed inside the cabin of an elevator, which allows positioning the LDA at any desired riser height.

Measurements are performed in the riser tube at heights close to the outlet. The three-component or 2-probe LDA data are recorded along the riser diameter at four angular positions marked with δ-angles (Figure 1) at eleven riser heights between 6.95 and 8.82 m.

Results and Discussion

Flow near the outlet

As previously mentioned the outlet section used in the current study consists of a blinded T-shaped tube (Figure 1). Such

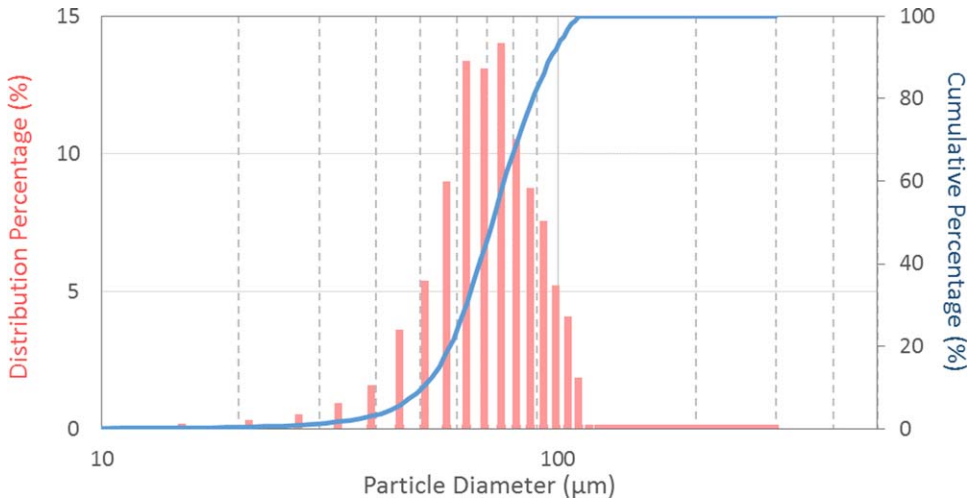

Figure 2. Volume histogram and cumulative distribution of the particle size of the FCC catalyst used.

Mean: 73.23 μm, Standard deviation: 17.73 μm, D10: 51.55 μm, D50: 72.78 μm, D90: 97.29 μm. [Color figure can be viewed in the online issue, which is available at wileyonlinelibrary.com.]

an outlet configuration is most commonly applied in industry as it reduces erosion due to particle impingement on the top riser wall.[29] The particles injected in the riser through the Y-shaped inlet at the bottom are entrained by the gas and ascend through the riser. As it was shown in a previous work,[39] the flow is fully developed at a height of about 2 m above the solids inlet. This fully developed gas-solid flow is maintained in the middle section of the riser,[39] but it gets disturbed when approaching the T-outlet, where air and particles leave the riser through the one-sided outlet tube. Because of the outlet geometry, the flow is forced to change direction and the streamlines should make a sharp turn into the 90° placed outlet tube. However, due to inertia as well as the locally developed centrifugal force, most of the particles will not directly leave the riser through the outlet tube, but continue flowing in nearly axial direction—with lower axial velocity—and hit the riser wall above the outlet tube, as also described in literature.[3,5,42] In the blinded tube of the riser outlet particles are then reflected to the wall opposite the outlet tube, losing most of their axial momentum. Under the influence of gravity the particles start falling along the riser wall opposite the outlet tube. As a result, a vortex is formed in the blinded extension of the T-outlet section. A reflux of solids is observed along the riser wall opposite the outlet tube, as visually observed (see Supporting Information Videos S1 and S2).

Particle flow characteristics

The outlet, as shown in Figure 1, forms an angle of 51° with the solids inlet. The figures below show the experimental data obtained at eleven different riser heights in the T-outlet configuration with an extension height of 0.1 m. In the figures presenting results of the experimental study as a function of dimensionless radius r/R, a positive r/R value corresponds with $\theta = \delta$, while a negative r/R value indicates that $\theta = \delta + 180°$, with δ referring to the probe position as presented in Figure 1. Using this convention the outlet opening is positioned at $\delta = 51°$ and $r/R = +1$, extending from a riser height of $z = 8.66$ m to 8.76 m. Although the extension height above the outlet opening is 0.1 m, the highest position where a measurement could be performed is $z = 8.82$ m, that is 0.06 m above the outlet opening.

Figure 3 shows the projections of the mean velocity, U, vectors on different axial planes in the riser outlet section for a volumetric air flow rate of 100 Nm^3/h. Remark that a lack of data at some angles and at given heights is either due to a lack of particles observed at that position or because the refraction of the laser beams on the riser wall ruins their alignment, that is, deforms the measuring volume. A vortex is clearly observed in the extension of the outlet (see Supporting Information Videos S1 and S2), as solids hit the riser wall just

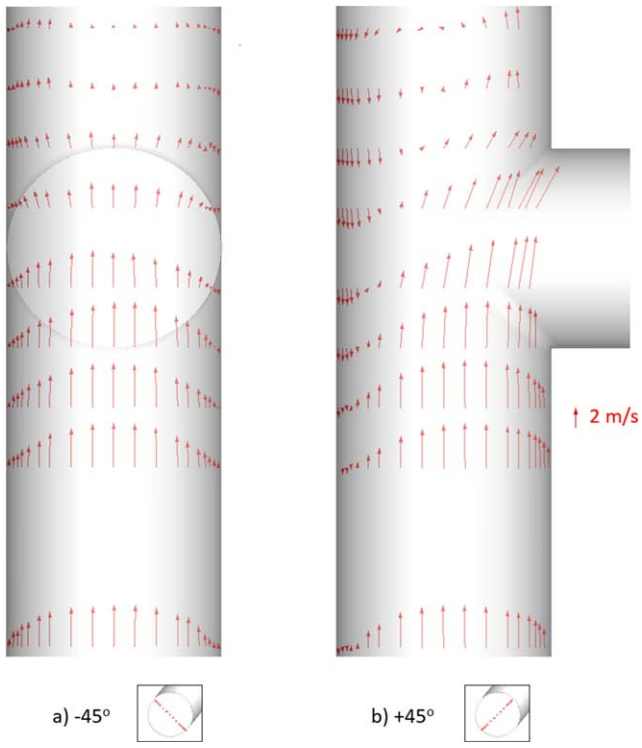

Figure 3. Projection of mean velocity vectors on different axial planes, 100 Nm^3/h for (a) $\delta = -45°$ and (b) $\delta = +45°$.

[Color figure can be viewed in the online issue, which is available at wileyonlinelibrary.com.]

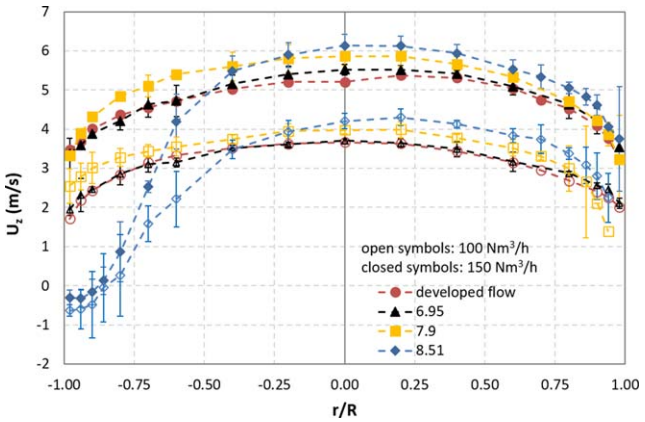

Figure 4. Mean axial particle velocities at $\delta = +45°$ for air flow rates of 100 Nm^3/h (open symbols) and 150 Nm^3/h (closed symbols).

Error bars represent the 95% confidence intervals based on three repeated experiments. The riser outlet extends from 8.66 to 8.76 m. Fully developed flow profiles from Pantzali et al.[39]. [Color figure can be viewed in the online issue, which is available at wileyonlinelibrary.com.]

above the outlet tube and are reflected toward the riser wall opposite to the outlet tube. The presence of a vortex is best observed when studying the axial velocity, U_z, profile at $\delta = +45°$ (Figure 4). There, the vortex formation is clearly seen to result in a recirculation of solids close to the riser wall opposite the outlet tube. The recirculation extends below the outlet tube (i.e., below 8.66 m) and is recorded up to the measuring position of $z = 8.51$ m. This means that the downflow extends to a height lower than the value reported by Van engelandt et al.,[17] which was 0.1 m below the outlet tube. The downflow velocity decreases with decreasing riser height (8.82 m $> z >$ 8.51 m). It will further diminish for riser heights between 8.51 and 7.9 m, as can be concluded from Figure 4. The axial velocities at $z = 7.9$ m are all positive. However, a flange on the riser tube obstructs the measurements in the range from 7.9 to 8.51 m. Thus, the downflow lower end cannot be defined more accurately and for the studied conditions it extends over a length of between 5 and 12% of the riser height. Lopes et al.[29] simulating an industrial riser with the same outlet configuration reported that the downflow can cover up to 28% of the riser total height.

It is observed that the height up to where the downflow extends, is fluctuating. A close observation of the velocity time series close to the edge of the downflow, i.e., at 8.51 m $< z <$ 8.66 m, $\delta = +45°$ and $-1 < r/R < -0.6$, shows that the particle descend (negative axial velocities in Figure 5a) is frequently interrupted by rising particles (positive axial velocities in Figure 5a). This results in an oscillation of the downflow lower end, evident in the Supporting Information Video S1 and S2, which causes the relatively large error bars for the axial velocity measurements (Figure 4). Statistical analysis (Figure 5b) of the velocity data collected at $\delta = +45°$ and $z = 8.51$ m indicates that in the downflow region the time and ensemble averages are not equal, indicating a nonergodicity phenomenon in this region. A study of all data in outlet section (present work), middle section,[39] and inlet section[40] of this riser shows that this behavior is observed in the downflow region only. As seen from Figure 5b the time and ensemble averages start converging ($r/R > -0.8$) and finally coincide ($r/R > -0.5$) when moving out of the downflow region. The skewness of the velocity data also indicates that the velocity distributions are asymmetric with respect to the mean value. In the downflow region a positive skewness of the velocity data shows that many recordings lie above the mean value, indicating the presence of rising particles as previously mentioned. Next to the downflow region, negative skewness shows that many velocity recordings are lower than the mean value. These recordings are related to particles—or possibly particle clusters—that rise with velocities lower than the majority of the other particles. Yet, all particles next to the downflow region are moving upwards, as no negative axial velocities are recorded.

Figure 4 indicates that the fully developed velocity profile recorded in the middle section of the riser[39] is obstructed starting from a riser height of about 7 m, that is, more than 1.5 m below the outlet opening, for both air flow rates of 100 Nm^3/h and 150 Nm^3/h, implying that the outlet effect is noticeable at the upper 20% riser part. At heights where downflow is recorded, the axial velocity profile is observed to be symmetrical with respect to the riser centerline only at $\delta = -45°$ (Figure 3a), as the plane is almost perpendicular to the outlet tube. Similar observations were made by De Wilde et al.[33] and Lopes et al.[29] The region of particles downflow decreases with increasing air flow. In other words, the downflow is restricted to higher riser heights with higher gas flow rate. An indication of this behavior is given in Figure 4, where the negative downflow velocities are diminished at $z = 8.51$ m for the higher flow rate. Chan et al.,[18] studying denser riser flows, reported

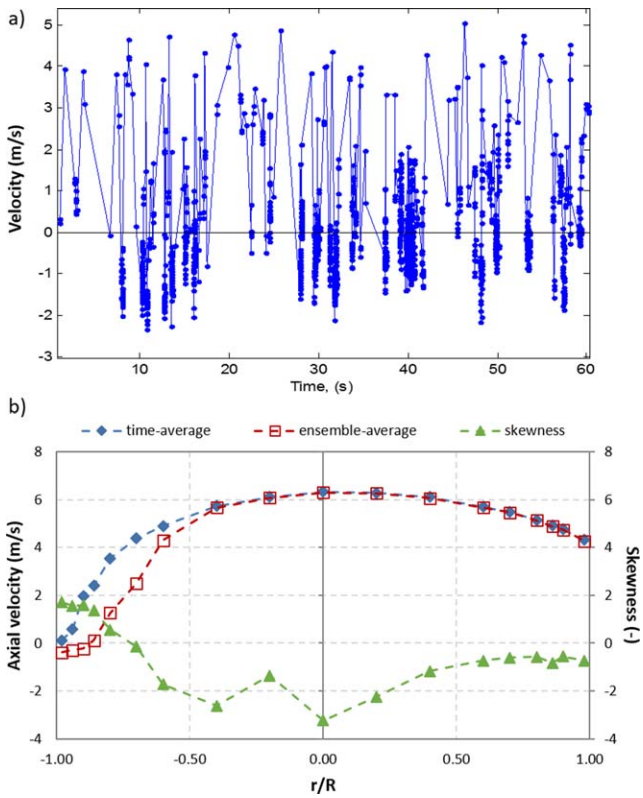

Figure 5. (a) Time series of the particle axial velocity recordings at 150 Nm^3/h, $\delta = +45°$, $z = 8.51$ m, r/R = −0.9. (b) Indicative statistical analysis of the solids axial components close to the edge of the downflow at 150 Nm^3/h, $\delta = +45°$, $z = 8.51$ m.

[Color figure can be viewed in the online issue, which is available at wileyonlinelibrary.com.]

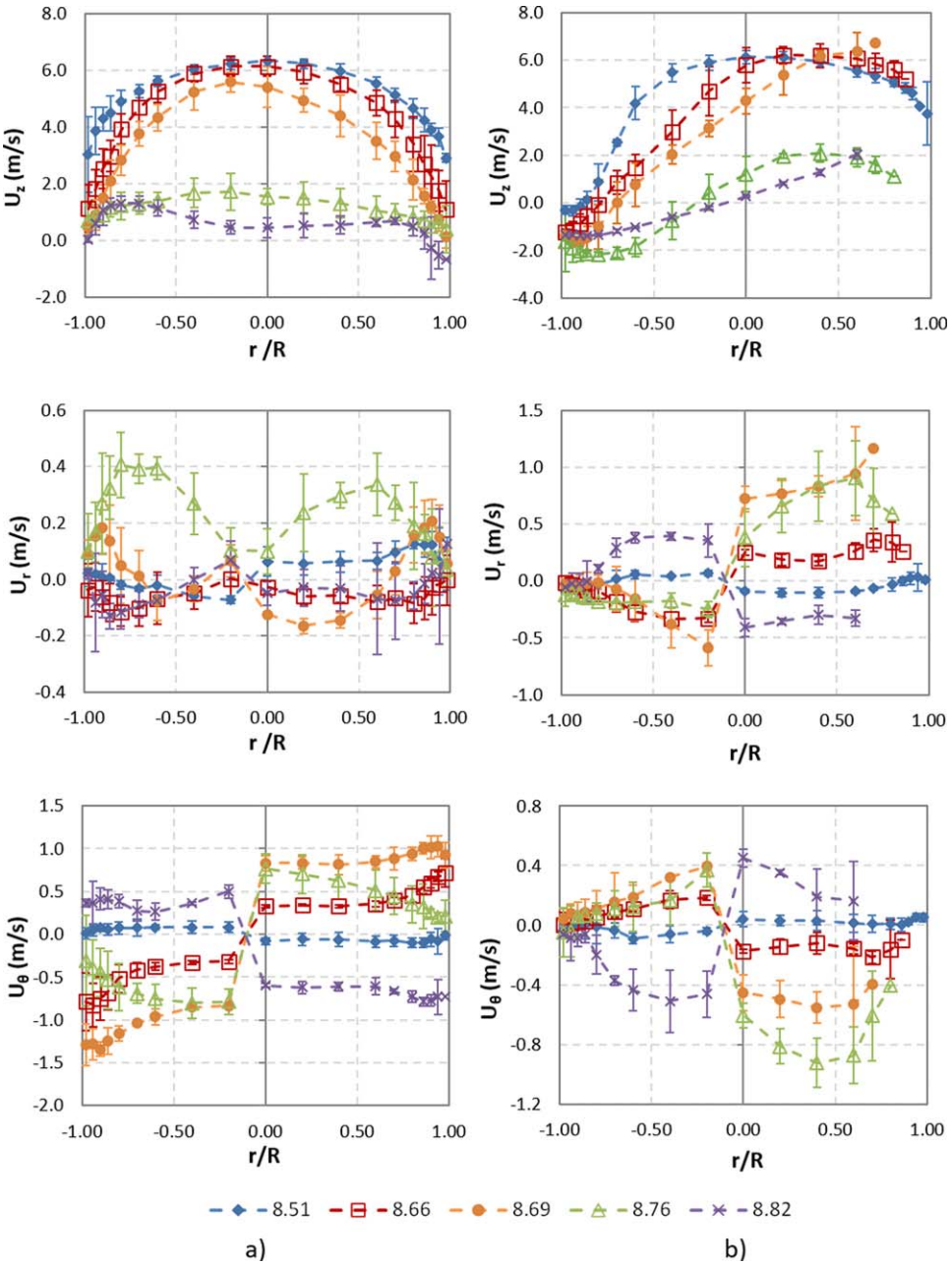

Figure 6. Mean axial, radial and azimuthal particle velocities for air flow rate of 150 Nm^3/h at (a) $\delta = -45°$ and (b) $\delta = +45°$.

Error bars represent the 95% confidence intervals based on three repeated experiments. The riser outlet extends from 8.66 to 8.76 m. [Color figure can be viewed in the online issue, which is available at wileyonlinelibrary.com.]

that particle velocities in the outlet region differ from those in the fully developed flow only at the lowest values of gas velocity and/or solids flow rate studied. In the present work it is seen that, although an increase in gas flow rate restricts the extent of the particle downflow region, the velocity profiles differ considerably from fully developed flow profiles for both gas flow rates studied (Figure 4). Furthermore, studies with both smooth and abrupt outlet configurations indicate a relevant deceleration of the particles as they approach the outlet.[16,43] In the present work, the mean particle velocity decreases due to the presence of the downflow region. However, as seen in Figure 4, the velocity of the rising particles is similar and sometimes even slightly higher as compared to the corresponding values in the fully developed flow region. The order of magnitude of the rising particle axial velocities is similar to the superficial gas velocity, a trend reported by Godfroy et al.[44] and Pantzali et al.[39] for the middle section of the riser.

As expected, the axial velocities are lower close to the walls due to wall friction. Except for $\delta = -45°$, the axial velocity profiles at all angles studied are not symmetrical with respect to the riser centerline ($r/R = 0$), which is in accordance with previous observations for denser flows.[9,16,18] This is clearly observed in Figure 6 where axial particle velocity profiles at the different measuring heights are presented for $\delta = -45°$ and $\delta = +45°$. Obviously this is due to the one-sided outlet geometry of the riser and to the resulting solids recirculation as discussed above. The axial velocity components are considerably larger than the corresponding radial, U_r, and azimuthal,

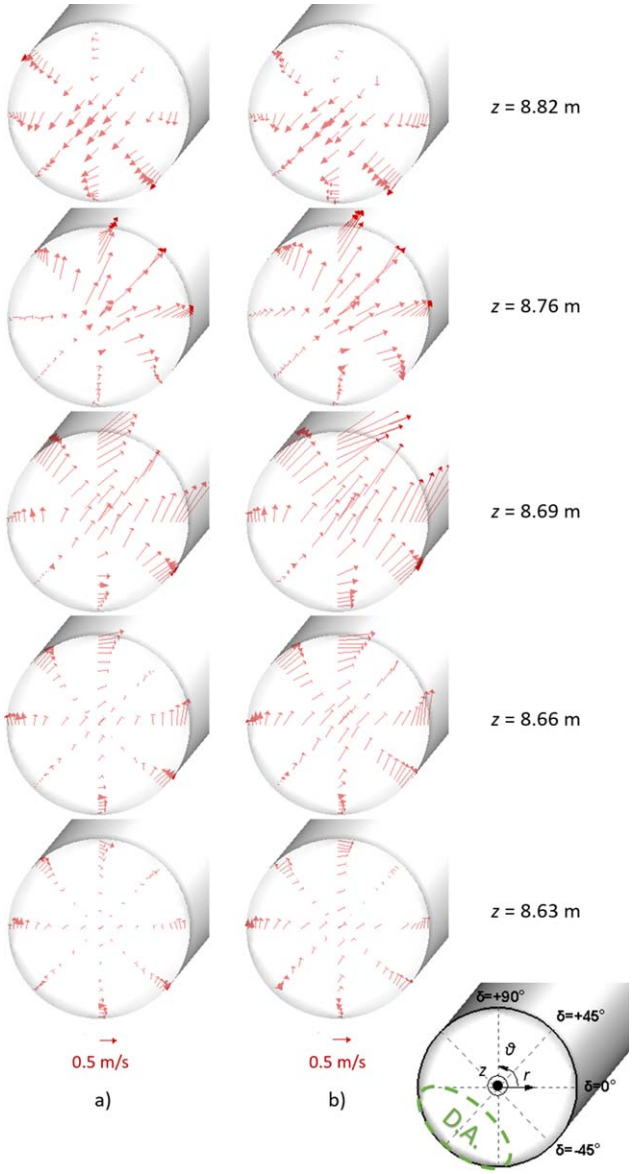

Figure 7. Particle velocity field in riser cross-sections at different heights for (a) 100 m^3/h and (b) 150 m^3/h.

The region of the downflow area (D.A.) is approximately indicated. The riser outlet extends from 8.66 to 8.76 m.[Color figure can be viewed in the online issue, which is available at wileyonlinelibrary.com.]

U_θ, velocities. The highest axial velocities are observed in front of the outlet tube, i.e., at $\delta = +45°$, $z = 8.69$ m and $r/R = 0.6$ due to the local acceleration. As particles move beyond that point toward the outlet, the axial velocity starts decreasing, as the geometrical configuration forces the particles to change direction. The radial velocities close to the upper half of the outlet tube ($r/R > 0$ and 8.69 m $\leq z \leq$ 8.76 m) are higher than the corresponding values close to the lower half of the outlet tube ($r/R>0$ and 8.66 m $\leq z <$ 8.69 m). Thus, the particles that enter the outlet tube have a higher velocity near the top wall of the outlet tube than near the bottom wall of the outlet tube. As a result, the stresses and erosion on the top wall of the outlet tube will be significantly more important. For a good understanding, it should be noted that the sudden change in the mean radial and azimuthal particle velocity components from positive to negative values (or vice versa) at the centerline of the riser ($r/R = 0$) in Figure 6 is a consequence of the cylindrical coordinate system. By definition, a negative mean radial particle velocity component implies that the flow is pointing toward the center of the riser tube. A positive value implies that the flow is pointing away from the center to the riser wall. Comparably, a positive mean azimuthal particle velocity component implies counterclockwise rotation, while a negative value implies clockwise rotation.

The cross-sectional flow is clearly represented by the vector plots in Figure 7. A general tendency of the particles in the downflow region is to flow toward the opposite riser walls. The radial velocities at $\delta = -45°$, that is the plane perpendicular to the outlet tube axis, show a slight trend of converging toward the riser center at lower riser heights and diverging from the riser center at higher riser positions. This can be more clearly observed in Figure 6a, where convergence or divergence with respect to the riser center is indicated by velocities of the same sign (all negative or positive respectively) over all r/R range. In other words, this means that at 8.66 m $< z <$ 8.69 m particles tend to move from the walls to the center of the riser as they move upwards. At $z >$ 8.69 m particles again disperse from the riser center toward the riser periphery. A similar, although more pronounced, behavior has been observed by Chew et al.[13] when measuring solids volume fraction profiles close to the outlet in a riser *of fluidized Geldart B particles*. Attributing this behavior to gas-phase turbulence effects[45] or to wall roughness[21] was found insufficient in the case of Chew et al.[13] They concluded that the reverse core annular pattern is also related to the high particle Stokes number, implying that the particles are not able to follow the gas streamlines and tend to diffuse toward the walls. Although the particles used in the present work are classified as Geldart A and hence have lower Stokes number than the Geldart B particles of Chew et al.,[13] a slight indication of reverse core-annular pattern is observed as previously described. However, this behavior could also be related to the presence of the downflow region, a consequence of the T-outlet. The resulting constriction of the cross-sectional area forces the rising flow of gas and particles to move toward the riser center. Azimuthal velocities at $\delta = -45°$ at the height of the riser outlet show the tendency of the particles to move toward the one-sided outlet tube (Figure 7). In the blinded tube of the T-outlet, where the vortex is created, the cross-sectional pattern changes completely, as the flow is redirected toward the riser wall opposite the outlet tube (Figure 7). Particles are observed to move away from the wall exactly above the outlet tube opening in both radial and azimuthal direction.

Figure 8 shows typical axial, u_z, radial, u_r, and azimuthal, u_θ, particle fluctuating velocities in the $\delta = +45°$ plane at different riser heights, for the two air flow rates studied. The particle fluctuating velocity is calculated as the standard deviation of the particle velocities. Axial fluctuating velocities are not symmetric over the riser diameter and vary significantly with the riser height in the outlet section of the riser. Three general trends for the axial fluctuating velocity profiles can be observed in the plane of the outlet tube axis ($\delta = +45°$) corresponding to heights below, along, and above the riser outlet. For riser heights below the outlet tube axis (i.e., $z <$ 8.71 m) high axial fluctuations are recorded close to the wall opposite the outlet tube, i.e., at $-0.9 < r/R < -0.5$. The maximum value gradually shifts toward the outlet tube, i.e., from $r/R = -0.8$ to $r/R = -0.6$, as the height increases. For $r/R > 0$

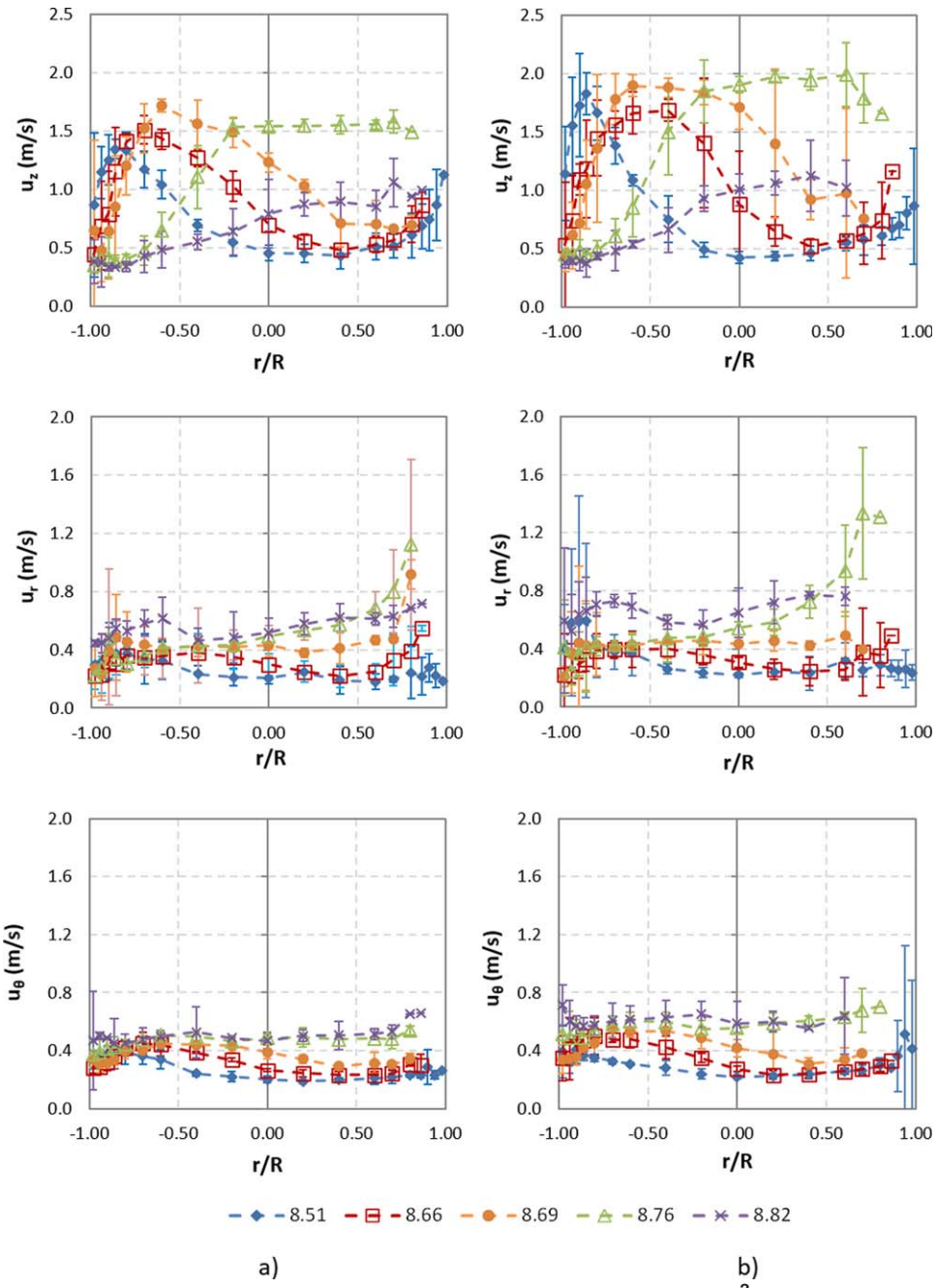

Figure 8. Particle fluctuating velocities for $\delta = +45^\circ$ and air flow rate of (a) 100 Nm^3/h and (b) 150 Nm^3/h.

Error bars represent the 95% confidence intervals based on three repeated experiments. The riser outlet extends from 8.66 to 8.76 m. [Color figure can be viewed in the online issue, which is available at wileyonlinelibrary.com.]

the axial fluctuations decrease significantly. The highest axial fluctuations are recorded at 8.69 m $< z <$ 8.76 m, that is at heights corresponding mostly to the upper half of the outlet tube opening. This can be explained by the change of flow direction of the particles from strongly axial to more radial as a consequence of the one sided outlet geometry of the riser. At these heights, the position of the highest axial fluctuation shifts from a radial position opposite the outlet tube, i.e., negative r/R at $z = 8.69$ m, toward the side of the outlet tube, i.e., positive r/R at $z = 8.76$ m. At heights in the blinded tube, $z > 8.76$ m, very different profiles are observed. Here, the highest axial fluctuations are recorded at positive r/R, i.e., above the outlet tube opening, and low values near the riser wall opposite the outlet tube opening. This is a consequence of the vortex and the downflow that are initiated above the outlet tube opening. Similar observations are made for both air flow rates. The azimuthal and radial fluctuating velocities are lower than the axial ones. They are in general observed to be higher in the downflow region of the riser, i.e., at negative r/R and $z < 8.79$ m, and also above the outlet tube opening where the vortex is created as seen in Figure 3, i.e., positive r/R and $z \geq 8.79$ m.

In Figure 9 the particle turbulence intensity, $I = |u/U|$, a measure for the turbulent fluctuations, is presented for the two flow rates studied. Despite the high error bars recorded, a peak in the turbulence intensity is observed at all measuring heights. Remark that very high values of the order of 400–800% are observed. The peaks indicate the lateral edge of the downflow

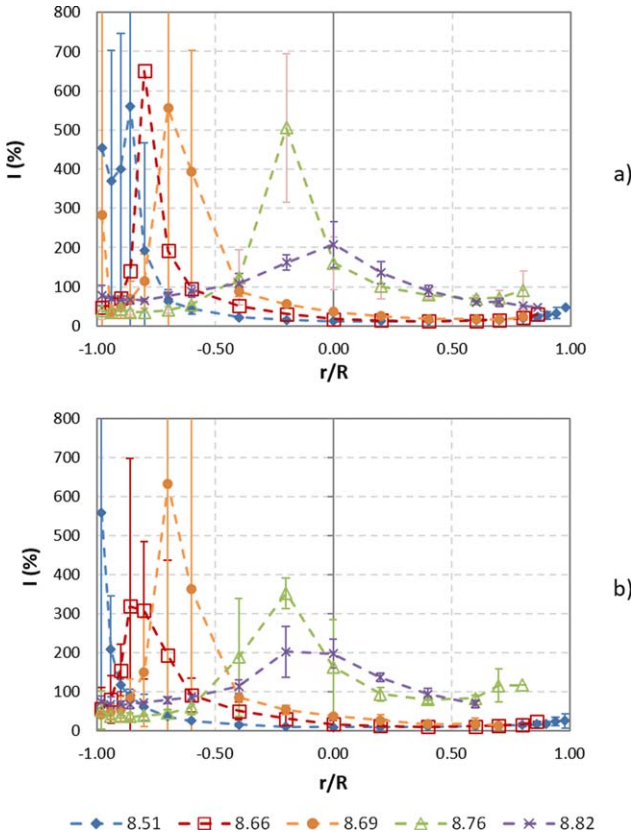

Figure 9. Turbulence intensity for $\delta = +45°$ and air flow rate of (a)100 Nm^3/h and (b) 150 Nm^3/h.

Error bars represent the 95% confidence intervals based on three repeated experiments. The riser outlet extends from 8.66 to 8.76 m. [Color figure can be viewed in the online issue, which is available at wileyonlinelibrary.com.]

region at each corresponding height, where the axial velocity turns from negative to positive values. Although root mean square (RMS) components do not exhibit a significant change at the specific radial positions, the axial mean velocity, the dominant velocity component (Figure 6), becomes zero, resulting in an overall decrease of the total solids velocity magnitude. Hence, the turbulence intensity shows a peak. The high error bar results from the slight oscillation of the downflow region edges as well as the slight errors due to the small offset in the probes position when performing repeated measurements. The turbulence intensity peak shifts from the center to the side opposite the outlet tube ($r/R < 0$) as the height decreases and the downflow becomes laterally more restricted and finally diminishes. Near the outlet tube the turbulence intensity decreases significantly, i.e., values of less than 100% are recorded.

The turbulence intensity trends can be explained based on the trends observed for the mean (Figure 6) and fluctuating (Figure 8) velocities. Below the outlet tube (8.51 m $< z <$ 8.66 m) the highest mean velocities are observed close to the core of the riser, while the lowest values are observed close to the wall opposite the outlet tube, where the downflow takes place (Figure 6). On the contrary, fluctuating velocities have their lowest values in the core of the riser and their higher values in the downflow region (Figure 8). Consequently, given its definition, turbulence intensity is high at the downflow region and decreases when moving toward the side of the outlet tube. Given that both fluctuating and mean velocities increase close to the outlet tube, the corresponding turbulence intensity values do not increase. In the blinded tube (8.76 m $< z <$ 8.82 m) a sharp peak in turbulence intensity is observed in the core of the riser. The lowest particle turbulence intensity is observed at the maximum height studied of $z = 8.82$ m. When comparing Figures 9a, b it is observed that the turbulence intensity at the lower air flow rate is somewhat higher than the corresponding values for the higher air flow rate. This is in accordance with observations of Van engelandt et al.[17]

The particle shear stresses τ_{rz} and $\tau_{z\theta}$ are calculated as $\tau_{ij} = \overline{u_i u_j}$ [39,40] using the corresponding particle fluctuations measured. The calculated values are then interpolated over three riser cross-sections. This allows visualizing how the shear stresses are distributed over a riser cross-section and how they change with riser height (Figure 10). In general the contours of shear stresses are symmetrical with respect to $\delta = +45°$, which is almost aligned with the outlet tube axis ($\delta = +51°$). At $z < 8.76$ m the τ_{rz} component (Figure 10b) is highest at an arc around the outlet tube axis located close to the riser wall opposite the outlet tube. The latter can be explained by the exchange between axial and radial momentum as the streamlines bend toward the outlet tube. The maximum values increase with riser height. Above $z = 8.76$ m, maximum τ_{rz} values are recorded at the semicircle above the outlet tube, where the solids by-passing the outlet tube hit the wall of the blinded tube, lose most of their momentum and are forced to recirculate. The $\tau_{z\theta}$ component (Figure 10a) acquires maximum values close to the walls aside of the outlet tube, indicating the local exchange between azimuthal and axial momentum. The $\tau_{z\theta}$ values increase with riser height as well up to $z = 8.76$ m.

In general, the observations of the present work cannot be generalized to any kind of abrupt outlet, because alterations, for example, in the outlet diameter or extension height, will have an effect on the flow pattern and solids velocities, as mentioned in literature,[5,7] although some studies claim this effect is limited.[2,30] The observation that flow patterns also depend on operating conditions and entire riser geometry explains these opposing statements.[30] It is questionable whether outlet effects are scaling effects, as many studies report that they are not observed in large scale units, while others prove that they can affect industrial scale risers as well.[38] More general conclusions on the effect of abrupt outlets can only be made either by collecting further experimental data, or by developing reliable computational models for risers and running systematic comparative case studies, varying just one operating condition/riser geometry detail at a time.

Conclusions

Coincident three component solids velocities are acquired for the first time in the T-outlet section of a 9 m-high pilot riser set-up, to study the hydrodynamics of a dilute gas-solid flow. Data were recorded at 11 riser heights between 6.95 and 8.82 m. The fully developed ascending gas-solid flow from the middle section of the riser gets disturbed by the outlet section at about 1.5 m below the outlet tube or in the upper 20% of the total riser height. The flow is decelerated when approaching the outlet tube, as the gas and solids are forced to change their flow direction to exit the riser. Nevertheless, due to inertia and the existence of the blinded tube above the outlet tube, most of the particles hit the riser wall above the outlet tube, get reflected to the opposite riser wall and fall due to gravity, creating a vortex. As a result, a downflow of solids is observed close to the riser wall opposite the outlet tube, which extends

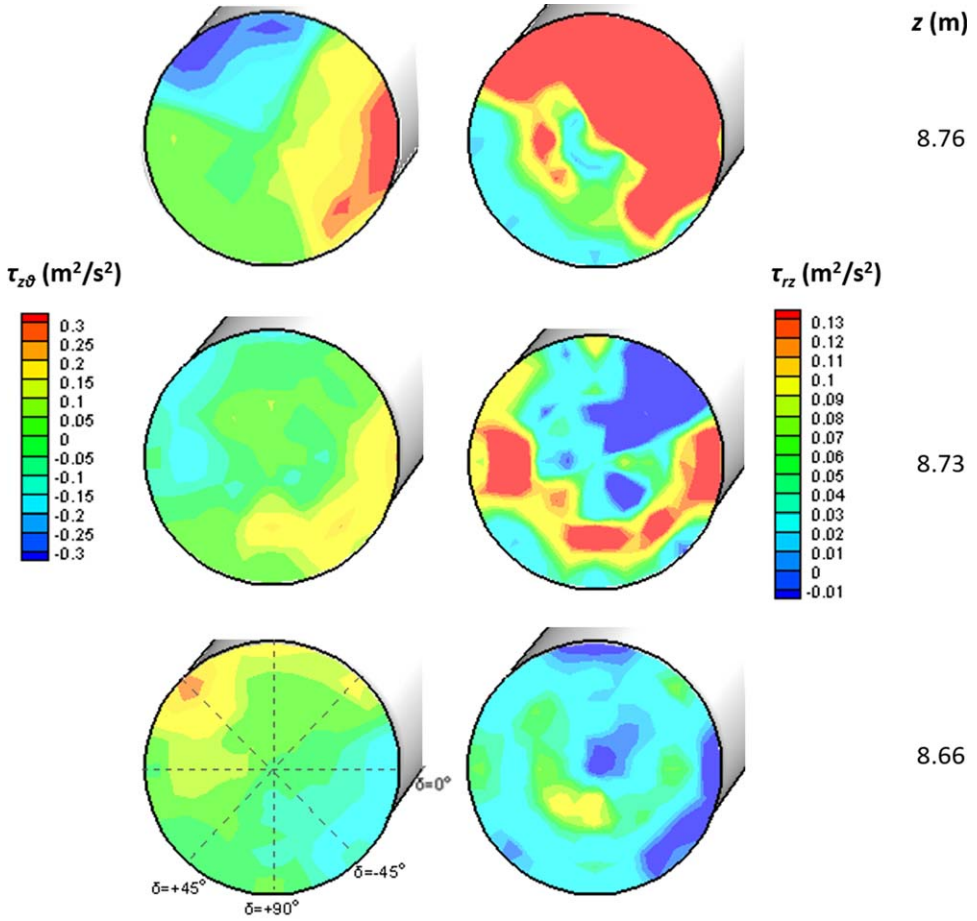

Figure 10. Reconstructed contour plot of (a) $\tau_{z\theta}$ and (b) τ_{rz} obtained based on interpolation of the experimental data at the height of the outlet tube for 100 Nm^3/h.

The riser outlet extends from 8.66 to 8.76 m. [Color figure can be viewed in the online issue, which is available at wileyonlinelibrary.com.]

below the outlet tube. The downflow is restricted to higher riser positions for higher gas flow rates.

A very detailed statistical analysis of the particle velocities is reported including turbulence intensities, isotropic coefficients and particle shear stresses, data which are scarce in literature for this kind of flow. In the downflow region of a riser a nonergodicity phenomenon is recorded, as time- and ensemble average velocities do not coincide. The skewness indicates that the velocity distributions are not symmetrical around the mean values. Radial particle velocities indicate a slight convergence of particles toward the riser center as solids approach the height of the outlet tube and a dispersion toward the riser walls and the outlet tube as soon as the outlet tube height is reached. Azimuthal particle velocities show the particle tendency to move toward the one-sided outlet tube. Particles entering the outlet tube have mostly higher velocities near the top wall of the outlet tube which will lead locally to higher stresses and erosion.

Velocity fluctuations mostly increase at heights corresponding to the outlet tube as well as the downflow region. Shear stresses become high at the areas where the flow direction changes; i.e., at an arc around the outlet tube axis and in the blinded tube where the vortex is formed. High turbulence intensity values are observed at the edges of the downflow region.

The presented experimental data combined with previous data obtained at different riser sections in the same pilot riser set-up and under the same operating conditions by Pantzali et al.[39] and by Pantzali et al.[40] give a full picture of the solids velocity field in the entire riser. A two-probe LDA provides the three components of the mean particle velocity vectors in dilute riser flow, thus offering more details and a better understanding of the physics of the flow and the flow development and at the same time a library of experimental data used for computational model validation.

Acknowledgments

This work was supported by the "Long Term Structural Methusalem Funding by the Flemish Government" and the European Research Council under the European Union's Seventh Framework Program FP7/2007-2013/ERC grant agreement n° 290793.

Notation

I = turbulence intensity, -
m = mass loading, -
r = radial coordinate, m
R = riser radius, m
S_{ij} = isotropic coefficient, -
U = mean particle velocity component, m/s
u = particle velocity fluctuation, m/s
z = axial coordinate, m
Z = riser height, m

Greek letters

δ = angle of the plane of measurements, °
ε_s = solids volume fraction, -
θ = azimuthal coordinate,
τ_{ij} = particle shear stress *ij* component, m^2/s^2

Subscripts

θ = azimuthal
i,j = indices of coordinate direction
r = radial
z = axial

Literature Cited

1. Gidaspow D, Jung J, Singh RK. Hydrodynamics of fluidization using kinetic theory: an emerging paradigm: 2002 Flour-Daniel lecture. *Powder Technol.* 2004;148(2–3):123–141.
2. Lackermeier U, Werther J. Flow phenomena in the exit zone of a circulating fluidized bed. *Chem Eng Process Process Intensif.* 2002; 41(9):771–783.
3. Bai DR, Jin Y, Yu ZQ, Zhu JX. The axial distribution of the cross-sectionally averaged voidage in fast fluidized beds. *Powder Technol.* 1992;71(1):51–58.
4. Cheng Y, Wei F, Yang G, Jin Y. Inlet and outlet effects on flow patterns in gas-solid risers. *Powder Technol.* 1998;98(2):151–156.
5. Gupta SK, Berruti F. Evaluation of the gas-solid suspension density in CFB risers with exit effects. *Powder Technol.* 2000;108(1):21–31.
6. Monazam ER, Breault RW, Shadle LJ. Pressure and apparent voidage profiles for riser with an abrupt exit (T-shape) in a CFB riser operating above fast fluidization regimes. *Powder Technol.* 2016; 291:383–391.
7. Zhang R, Yang H, Wu Y, Zhang H, Lu J. Experimental study of exit effect on gas–solid flow and heat transfer inside CFB risers. *Exp Therm Fluid Sci.* 2013;51:291–296.
8. Wang X, Liao L, Fan B, Jiang F, Xu X, Wang S, Xiao Y. Experimental validation of the gas-solid flow in the CFB riser. *Fuel Process Technol.* 2010;91(8):927–933.
9. Yan A, Pärssinen JH, Zhu J-X. Flow properties in the entrance and exit regions of a high-flux circulating fluidized bed riser. *Powder Technol.* 2003;131(2–3):256–263.
10. van der Meer EH, Thorpe RB, Davidson JF. Flow patterns in the square cross-section riser of a circulating fluidised bed and the effect of riser exit design. *Chem Eng Sci.* 2000;55(19):4079–4099.
11. Pugsley T, Lapointe D, Hirschberg B, Werther J. Exit effects in circulating fluidized bed risers. *Can J Chem Eng.* 1997;75(6):1001–1010.
12. Kim J-S, Tachino R, Tsutsumi A. Effects of solids feeder and riser exit configuration on establishing high density circulating fluidized beds. *Powder Technol.* 2008;187(1):37–45.
13. Chew JW, Hays R, Findlay JG, et al. Reverse core-annular flow of Geldart Group B particles in risers. *Powder Technol.* 2012;221:1–12.
14. Chew JW, Parker DM, Cocco RA, Hrenya CM. Cluster characteristics of continuous size distributions and binary mixtures of Group B particles in dilute riser flow. *Chem Eng J.* 2011;178(0):348–358.
15. Chew JW, Hays R, Findlay JG, et al. Cluster characteristics of Geldart Group B particles in a pilot-scale CFB riser. I. Monodisperse systems. *Chem Eng Sci.* 2012;68(1):72–81.
16. Zhou J, Grace JR, Lim CJ, Brereton CMH. Particle velocity profiles in a circulating fluidized bed riser of square cross-section. *Chem Eng Sci.* 1995;50(2):237–244.
17. Van engelandt G, Heynderickx GJ, De Wilde J, Marin GB. Experimental and computational study of T- and L-outlet effects in dilute riser flow. *Chem Eng Sci.* 2011;66(21):5024–5044.
18. Chan CW, Brems A, Mahmoudi S, et al. PEPT study of particle motion for different riser exit geometries. *Particuology.* 2010;8(6):623–630.
19. Van de Velden M, Baeyens J, Seville JPK, Fan X. The solids flow in the riser of a circulating fluidised bed (CFB) viewed by positron emission particle tracking (PEPT). *Powder Technol.* 2008;183(2):290–296.
20. Panday R, Breault R, Shadle LJ. Dynamic modeling of the circulating fluidized bed riser. *Powder Technol.* 2016;291:522–535.
21. Benyahia S, Syamlal M, O'Brien TJ. Study of the ability of multiphase continuum models to predict core-annulus flow. *AlChE J.* 2007;53(10):2549–2568.
22. van der Hoef MA, van Sint Annaland M, Deen NG, Kuipers JAM. Numerical simulation of dense gas-solid fluidized beds: a multiscale modeling strategy. *Annu Rev Fluid Mech.* 2008;40(1):47–70.
23. Andrews, Loezos PN, Sundaresan S. Coarse-grid simulation of gas-particle flows in vertical risers. *Ind Eng Chem Res.* 2005;44(16): 6022–6037.
24. Berruti F, Pugsley TS, Godfroy L, Chaouki J, Patience GS. Hydrodynamics of circulating fluidized bed risers: a review. *Can J Chem Eng.* 1995;73(5):579–602.
25. Huilin L, Gidaspow D, Bouillard J, Wentie L. Hydrodynamic simulation of gas-solid flow in a riser using kinetic theory of granular flow. *Chem Eng J.* 2003;95(1–3):1–13.
26. Almuttahar A, Taghipour F. Computational fluid dynamics of high density circulating fluidized bed riser: study of modeling parameters. *Powder Technol.* 2008;185(1):11–23.
27. Mathiesen V, Solberg T, Arastoopour H, Hjertager BH. Experimental and computational study of multiphase gas/particle flow in a CFB riser. *AlChE J.* 1999;45(12):2503–2518.
28. Benyahia S, Arastoopour H, Knowlton TM, Massah H. Simulation of particles and gas flow behavior in the riser section of a circulating fluidized bed using the kinetic theory approach for the particulate phase. *Powder Technol.* 2000;112(1–2):24–33.
29. Lopes GC, Rosa LM, Mori M, Nunhez JR, Martignoni WP. CFD study of industrial FCC risers: the effect of outlet configurations on hydrodynamics and reactions. *Int J Chem Eng.* 2012;2012:16.
30. Zhao B, Zhou Q, Wang J, Li J. CFD study of exit effect of high-density CFB risers with EMMS-based two-fluid model. *Chem Eng Sci.* 2015;134:477–488.
31. Shi X, Wu Y, Lan X, Liu F, Gao J. Effects of the riser exit geometries on the hydrodynamics and solids back-mixing in CFB risers: 3D simulation using CPFD approach. *Powder Technol.* 2015;284:130–142.
32. Wu X, Jiang F, Xu X, Xiao Y. CFD simulation of smooth and T-abrupt exits in circulating fluidized bed risers. *Particuology.* 2010; 8(4):343–350.
33. De Wilde J, Marin GB, Heynderickx GJ. The effects of abrupt T-outlets in a riser: 3D simulation using the kinetic theory of granular flow. *Chem Eng Sci.* 2003;58(3–6):877–885.
34. Das AK, De Wilde J, Heynderickx GJ, Marin GB. CFD simulation of dilute phase gas-solid riser reactors: part II-simultaneous adsorption of SO_2-NO_x from flue gases. *Chem Eng Sci.* 2004;59(1):187–200.
35. Rao A, Curtis JS, Hancock BC, Wassgren C. Numerical simulation of dilute turbulent gas-particle flow with turbulence modulation. *AlChE J.* 2012;58(5):1381–1396.
36. Benyahia S, Syamlal M, O'Brien TJ. Evaluation of boundary conditions used to model dilute, turbulent gas/solids flows in a pipe. *Powder Technol.* 2005;156(2–3):62–72.
37. Passalacqua A, Fox RO. Advanced continuum modelling of gas-particle flows beyond the hydrodynamic limit. *Appl Math Model.* 2011;35(4):1616–1627.
38. Van engelandt G, De Wilde J, Heynderickx GJ, Marin GB. Experimental study of inlet phenomena of 35° inclined non-aerated and aerated Y-inlets in a dilute cold-flow riser. *Chem Eng Sci.* 2007;62(1–2):339–355.
39. Pantzali MN, Lozano Bayón N, Heynderickx GJ, Marin GB. Three-component solids velocity measurements in the middle section of a riser. *Chem Eng Sci.* 2013;101:412–423.
40. Pantzali MN, De Ceuster B, Marin GB, Heynderickx GJ. Three-component particle velocity measurements in the bottom section of a riser. *Int J Multiphase Flow.* 2015;72(0):145–154.
41. Geldart D. Types of gas fluidization. *Powder Technol.* 1973;7(5): 285–292.
42. Harris AT, Davidson JF, Thorpe RB. Influence of exit geometry in circulating fluidized-bed risers. *AlChE J.* 2003;49(1):52–64.
43. Pärssinen JH, Zhu JX. Particle velocity and flow development in a long and high-flux circulating fluidized bed riser. *Chem Eng Sci.* 2001;56(18):5295–5303.
44. Godfroy L, Larachi F, Chaouki J. Position and velocity of a large particle in a gas solid riser using the radioactive particle tracking technique. *Can J Chem Eng.* 1999;77(2):253–261.
45. Bolio EJ, Yasuna JA, Sinclair JL. Dilute turbulent gas-solid flow in risers with particle-particle interactions. *AlChE J.* 1995;41(6):1375–1388.

Manuscript received Jan. 7, 2016, and revision received Mar. 15, 2016.